# *Ab initio* four-body calculation of $n$-$^3$He, $p$-$^3$H, and $d$-$d$ scattering

A. Deltuva* and A. C. Fonseca
*Centro de Física Nuclear da Universidade de Lisboa, P-1649-003 Lisboa, Portugal*
(Received March 8, 2007)

Four-body equations in momentum space are solved for neutron-$^3$He, proton-$^3$H, and deuteron-deuteron scattering; all three reactions are coupled. The Coulomb interaction between the protons is included using the screening and renormalization approach as it was recently done for proton-deuteron and proton-$^3$He scattering. Realistic interactions are used between nucleon pairs. For the first time fully converged results for the observables pertaining to the six different elastic and transfer reactions are obtained and compared with experimental data.

PACS numbers: 21.30.-x, 21.45.+v, 24.70.+s, 25.10.+s



Modern studies of nuclear structure and reactions require *ab initio* calculations of the quantum many-body system using realistic interactions. While at present there is a number of successful *ab initio* structure calculations using Green's function Monte Carlo (GFMC) methods [1, 2] and No Core Shell Model [3], *ab initio* studies of nuclear reactions are still limited to few specific few-nucleon reactions. The difficulties associated with the treatment of the long range Coulomb interaction restricted, until recently, precise calculations to neutron-deuteron ($n$-$d$) elastic scattering and breakup [4], and proton-deuteron ($p$-$d$) [5], $n$-$^3$H [6] and $p$-$^3$He [7] elastic scattering at low energy. The situation has now changed due to the work in Ref. [8]. Using the ideas of screening and renormalization [9] fully converged results for observables in $p$-$d$ elastic scattering and breakup were obtained for a wide range of energies and configurations using realistic force models. Other developments took place recently using the GFMC's approach [10] to calculate the $n$-$^4$He phase shifts at energies well below the inelastic threshold.

In the present work we attempt to further extend *ab initio* calculations of the four-nucleon ($4N$) system by solving the Alt, Grassberger and Sandhas (AGS) equations [11] for the $n$-$^3$He, $p$-$^3$H and $d$-$d$ reactions. This is the most complex scattering calculation that has been attempted so far since all three reactions are coupled and involve both isospin $\mathcal{T} = 0$ and $\mathcal{T} = 1$ states, together with a very small admixture of $\mathcal{T} = 2$ due to the charge dependence of the hadronic and electromagnetic interactions. This work is the continuation of two previous works for $n$-$^3$H [12] and $p$-$^3$He [13] where the $4N$ scattering problem was calculated with the same level of accuracy as it already exists for three-nucleon ($3N$) system. This means that calculations are carried out without approximations on the two-nucleon ($2N$) transition matrix (t-matrix) like in Ref. [14] or limitations on the choice of basis functions as in Ref. [15]. Therefore, after partial wave decomposition, the AGS equations are three-variable integral equations that are solved numerically without any approximations beyond the usual discretization of continuum variables on a finite momentum mesh. Therefore discrepancies with data may be attributed solely to the underlying $2N$ forces or lack of $3N$ forces.

The equations we solve are based on the symmetrized four-body AGS equations of Ref. [12]. In order to include the Coulomb interaction we follow the methodology of Refs. [8, 13] and add to the nuclear $pp$ potential the screened Coulomb one $w_R$ that, in configuration space, is given by

$$w_R(r) = w(r)\, e^{-(r/R)^n}, \tag{1}$$

where $w(r) = \alpha_e/r$ is the true Coulomb potential, $\alpha_e \simeq 1/137$ is the fine structure constant, and $n$ controls the smoothness of the screening; $n = 4$ to 8 are the optimal values that ensure that $w_R(r)$ approximates well $w(r)$ for $r < R$ and simultaneously vanishes rapidly for $r > R$, providing a comparatively fast convergence of the partial-wave expansion. The screening radius $R$ must be considerably larger than the range of the strong interaction but from the point of view of scattering theory $w_R$ is still of short range. Therefore the equations of Ref. [12] become $R$ dependent. The transition operators $\mathcal{U}^{\alpha\beta}_{(R)}$ where $\alpha(\beta) = 1$ and 2 corresponds to initial/final $1+3$ and $2+2$ two-cluster states, respectively, satisfy the symmetrized AGS equations

$$\begin{aligned}\mathcal{U}^{11}_{(R)} = & -(G_0\, t^{(R)} G_0)^{-1} P_{34} - P_{34}\, U^1_{(R)}\, G_0\, t^{(R)} G_0\, \mathcal{U}^{11}_{(R)} \\ & + U^2_{(R)} G_0\, t^{(R)} G_0\, \mathcal{U}^{21}_{(R)}, \end{aligned} \tag{2a}$$

$$\begin{aligned}\mathcal{U}^{21}_{(R)} = & (G_0\, t^{(R)} G_0)^{-1}\, (1 - P_{34}) \\ & + (1 - P_{34}) U^1_{(R)}\, G_0\, t^{(R)} G_0\, \mathcal{U}^{11}_{(R)} \end{aligned} \tag{2b}$$

for $1 + 3$ as the initial state and

$$\begin{aligned}\mathcal{U}^{12}_{(R)} = & (G_0\, t^{(R)} G_0)^{-1} - P_{34}\, U^1_{(R)}\, G_0\, t^{(R)} G_0\, \mathcal{U}^{12}_{(R)} \\ & + U^2_{(R)} G_0\, t^{(R)} G_0\, \mathcal{U}^{22}_{(R)}, \end{aligned} \tag{3a}$$

$$\mathcal{U}^{22}_{(R)} = (1 - P_{34}) U^1_{(R)}\, G_0\, t^{(R)} G_0\, \mathcal{U}^{12}_{(R)} \tag{3b}$$

for $2 + 2$ as the initial state. In both sets of equations $G_0$ is the four free particle Green's function and $t^{(R)}$ the $2N$ t-matrix derived from nuclear potential plus screened

Coulomb between $pp$ pairs. The operators $U^{\alpha}_{(R)}$ obtained from

$$U^{\alpha}_{(R)} = P_\alpha G_0^{-1} + P_\alpha\, t^{(R)}\, G_0\, U^{\alpha}_{(R)}, \tag{4a}$$

$$P_1 = P_{12}\, P_{23} + P_{13}\, P_{23}, \tag{4b}$$

$$P_2 = P_{13}\, P_{24}, \tag{4c}$$

are the symmetrized AGS operators for the $1+(3)$ and $(2)+(2)$ subsystems and $P_{ij}$ is the permutation operator of particles $i$ and $j$. Defining the initial/final $1+(3)$ and $(2)+(2)$ states with relative two-body momentum $\mathbf{p}$

$$|\phi^{(R)}_\alpha(\mathbf{p})\rangle = G_0\, t^{(R)} P_\alpha |\phi^{(R)}_\alpha(\mathbf{p})\rangle, \tag{5}$$

the amplitudes for all possible two-cluster transitions are obtained as $\langle \mathbf{p}_f|T^{\alpha\beta}_{(R)}|\mathbf{p}_i\rangle = S_{\alpha\beta}\langle\phi^{(R)}_\alpha(\mathbf{p}_f)|\mathcal{U}^{\alpha\beta}_{(R)}|\phi^{(R)}_\beta(\mathbf{p}_i)\rangle$ with $S_{11}=3$, $S_{21}=\sqrt{3}$, $S_{22}=2$ and $S_{12}=2\sqrt{3}$.

In close analogy with $p$-$d$ elastic scattering, the full scattering amplitude, when calculated between initial and final $p$-$^3$H or $d$-$d$ states, may be decomposed as follows

$$T^{\alpha\beta}_{(R)} = t^{\rm c.m.}_{\alpha R}\ \delta_{\alpha\beta} + [T^{\alpha\beta}_{(R)} - t^{\rm c.m.}_{\alpha R}\ \delta_{\alpha\beta}], \tag{6}$$

with the long-range part $t^{\rm c.m.}_{\alpha R}$ being the two-body t-matrix derived from the screened Coulomb potential of the form (1) between the proton and the center of mass (c.m.) of $^3$H for $\alpha=1$ and between the c.m. of both deuterons for $\alpha=2$. The remaining is the Coulomb-distorted short-range part $[T^{\alpha\beta}_{(R)} - t^{\rm c.m.}_{\alpha R}\ \delta_{\alpha\beta}]$ as demonstrated in Refs. [9, 16]. Applying the renormalization procedure, i.e., multiplying both sides of Eq. (6) by the renormalization factors $[Z^{\alpha}_R]^{-\frac{1}{2}}$ on the left and $[Z^{\beta}_R]^{-\frac{1}{2}}$ on the right [8, 9], in the $R\to\infty$ limit, yields the full transition amplitude in the presence of Coulomb

$$\langle \mathbf{p}_f|T^{\alpha\beta}|\mathbf{p}_i\rangle = \langle \mathbf{p}_f|t^{\rm c.m.}_{\alpha C}|\mathbf{p}_i\rangle\ \delta_{\alpha\beta} + \lim_{R\to\infty}\Big\{[Z^{\alpha}_R]^{-\frac{1}{2}} \times \langle \mathbf{p}_f|[T^{\alpha\beta}_{(R)} - t^{\rm c.m.}_{\alpha R}\ \delta_{\alpha\beta}]|\mathbf{p}_i\rangle [Z^{\beta}_R]^{-\frac{1}{2}}\Big\}, \tag{7}$$

where the $[Z^{\alpha}_R]^{-1}\langle \mathbf{p}_f|t^{\rm c.m.}_{\alpha R}|\mathbf{p}_i\rangle$ converges (in general, as a distribution) to the exact Coulomb amplitude $\langle \mathbf{p}_f|t^{\rm c.m.}_{\alpha C}|\mathbf{p}_i\rangle$ between the proton and the c.m. of the $^3$H nucleus (between the c.m. of both deuterons) and therefore is replaced by it. The renormalization factor is employed in the partial-wave dependent form as in Refs. [8, 13]

$$Z^{\alpha}_R = e^{-2i(\sigma^{\alpha}_L - \eta^{\alpha}_{LR})} \tag{8}$$

with the diverging screened Coulomb $p$-$^3$H ($d$-$d$) phase shift $\eta^{\alpha}_{LR}$ corresponding to standard boundary conditions and the proper Coulomb one $\sigma^{\alpha}_L$ referring to the logarithmically distorted proper Coulomb boundary conditions. Obviously, there is no long-range Coulomb force in the

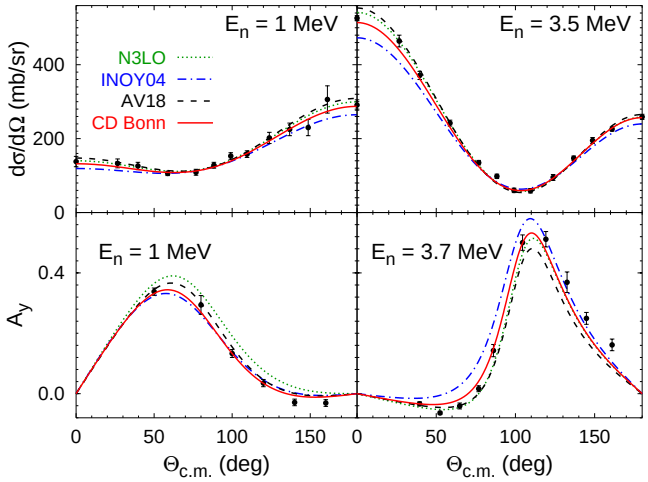


FIG. 1: (Color online) Differential cross section and neutron analyzing power of elastic $n$-$^3$He scattering at 1, 3.5, and 3.7 MeV neutron lab energy. Results obtained with potentials CD Bonn (solid curves), AV18 (dashed curves), INOY04 (dashed-dotted curves), and N3LO (dotted curves) are compared. The cross section data are from Ref. [21], $A_y$ data are from Ref. [22] at 1 MeV and from Ref. [23] at 3.7 MeV.

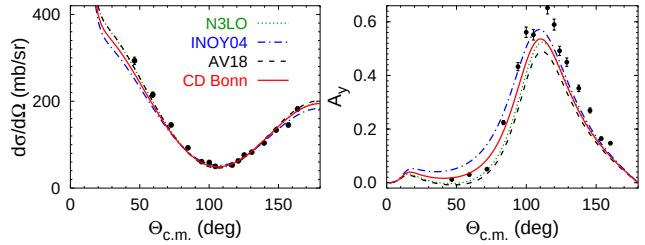


FIG. 2: (Color online) Differential cross section and proton analyzing power of elastic $p$-$^3$H scattering at 4.15 MeV proton lab energy. Curves as in Fig. 1. The data are from Ref. [24].

$n$-$^3$He states; in that case $\langle \mathbf{p}_f|t^{\rm c.m.}_{\alpha C}|\mathbf{p}_i\rangle = \langle \mathbf{p}_f|t^{\rm c.m.}_{\alpha R}|\mathbf{p}_i\rangle = 0$, and $\sigma^{\alpha}_L = \eta^{\alpha}_{LR} = 0$. The second term in Eq. (7), after renormalization by $[Z^{\alpha}_R]^{-\frac{1}{2}}\ [Z^{\beta}_R]^{-\frac{1}{2}}$, represents the Coulomb-modified nuclear short-range amplitude. It has to be calculated numerically, but, due to its short-range nature, the $R\to\infty$ limit is reached with sufficient accuracy at finite screening radii $R$ as demonstrated in Refs. [8, 13] for $p$-$d$ and $p$-$^3$He scattering. As found there, one needs larger values of $R$ at lower energies, making the convergence of the results more difficult to reach. Nevertheless, for $E_p > 1$ MeV or $E_d > 1$ MeV the method leads to very precise results. Depending on the reaction and the energy, we obtain fully converged results for $n$-$^3$He, $p$-$^3$H, and $d$-$d$ observables with $R$ ranging from 10 to 20 fm.

The results are also fully converged with respect to the partial-wave expansion. The calculations include isospin-singlet $2N$ partial waves with total angular momentum

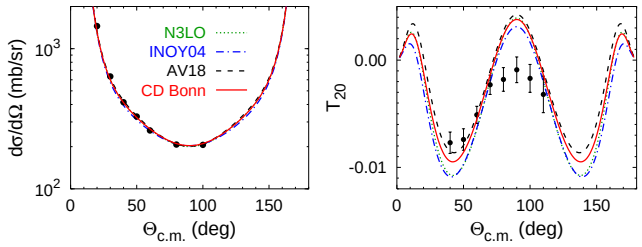


FIG. 3: (Color online) Differential cross section and deuteron tensor analyzing power $T_{20}$ of elastic $d$-$d$ scattering at 3 MeV deuteron lab energy. Curves as in Fig. 1. The cross section data are from Ref. [25] and $T_{20}$ data are from Ref. [26].

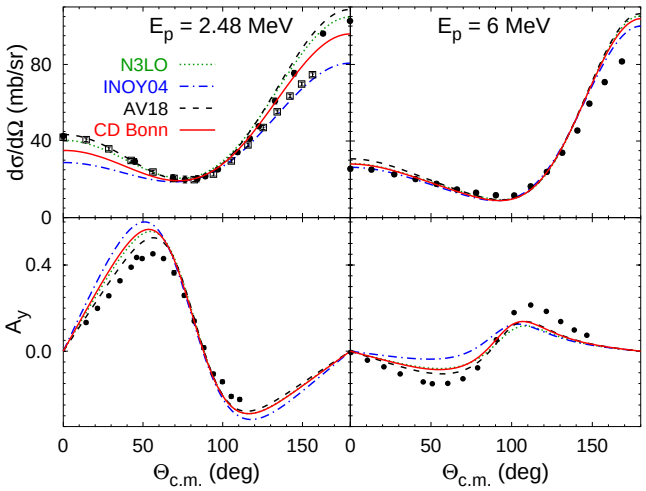


FIG. 4: (Color online) Differential cross section and proton analyzing power of $p + {}^3\mathrm{H} \to n + {}^3\mathrm{He}$ reaction at 2.48 and 6 MeV proton lab energy. Curves as in Fig. 1. The cross section data are from Refs. [27] (circles) and [28] (squares) at 2.48 MeV, and from Ref. [29] at 6 MeV. $A_y$ data are from Ref. [30] at 2.48 MeV and from Ref. [31] at 6 MeV.

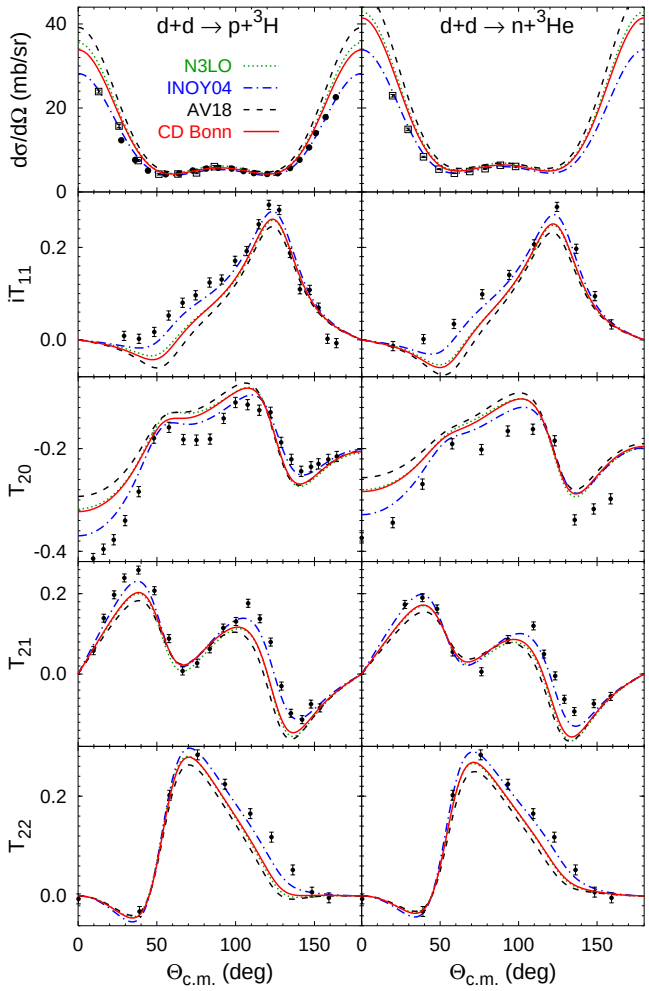


FIG. 5: (Color online) Differential cross section and deuteron analyzing powers of $d + d \to p + {}^3\mathrm{H}$ and $d + d \to n + {}^3\mathrm{He}$ reactions at 3 MeV deuteron lab energy. Curves as in Fig. 1. The cross section data are from Refs. [32] (squares) and [33] (circles). Analyzing power data are from Ref. [33] for $d+d \to p + {}^3\mathrm{H}$ and from Ref. [34] for $d + d \to n + {}^3\mathrm{He}$.

$I \leq 4$ and isospin-triplet $2N$ partial waves with orbital angular momentum $l_x \leq 6$, $3N$ partial waves with spectator orbital angular momentum $l_y \leq 6$ and total angular momentum $J \leq \frac{13}{2}$, $4N$ partial waves with 1+3 and 2+2 orbital angular momentum $l_z \leq 6$, resulting up to about 15000 channels for fixed $4N$ total angular momentum and parity. Initial/final two-cluster states with orbital angular momentum $L \leq 5$ are included for the calculation of observables. For some reactions, e.g., $n$-$^3$He elastic scattering, the partial-wave convergence is considerably faster, allowing for a reduction in the employed angular momentum cutoffs.

The two-nucleon interactions we use are charge-dependent (CD) Bonn [17], AV18 [18], inside nonlocal outside Yukawa (INOY04) potential by Doleschall [19], and the one derived from chiral perturbation theory at next-to-next-to-next-to-leading order (N3LO) [20]. In Figs. 1 through 5 we show the results for six different reactions. The most remarkable findings are: a) the excellent agreement with the data for the calculated $d$-$d$ elastic differential cross section; b) the lack of a large $A_y$ deficiency in $n$-$^3$He and $p$-$^3$H unlike what was observed before in $p$-$^3$He [13, 15]; c) the overall description of $d + d \to n + {}^3\mathrm{He}$ and $d + d \to p + {}^3\mathrm{H}$ data, given its complex structure.

Of all the potentials we use only INOY04 represents both $n$-$^3$He and $p$-$^3$H thresholds in the correct position (-7.72 MeV and -8.48 MeV, respectively). For this reason it is perhaps not surprising to see that this potential gives rise to the best description of $d + d \to n + {}^3\mathrm{He}$ and $d + d \to p + {}^3\mathrm{H}$ data, including the differential cross section. Nevertheless, even if the correct position of thresholds is an important factor, it is certainly not the only one that matters since in $n$-$^3$He elastic scattering and $p + {}^3\mathrm{H} \to$

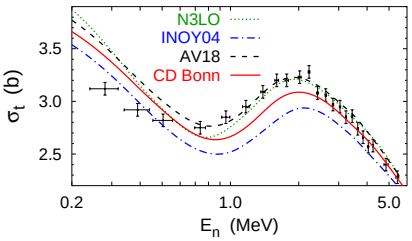


FIG. 6: (Color online) $n$-$^3$He total cross section as function of the neutron lab energy. Curves as in Fig. 1. The data are from Ref. [35].

$n+^3$He INOY04 gives rise to results that are poorer than those obtained with other potentials.

The largest disagreements with data are observed in a very small $d$-$d$ elastic $T_{20}$ at 90°, and in the $p + {}^3\mathrm{H} \to n+{}^3\mathrm{He}$ proton analyzing power and differential cross section at forward and backward angles at low energies. At $E_p = 2.48$ MeV we find two sets of data that are inconsistent at backward angles but where this work does not help to resolve given the wide range of results obtained with the potentials we use. At $E_p = 6$ MeV the results are almost independent of the choice of potentials but they all miss the data at backward angles. The problems associated with $n$-$^3$He and $p$-$^3$H reactions may be associated with the $0^+$ excited state of the alpha particle that sits between the two thresholds and whose position changes with the potential we choose.

Finally in Fig. 6 we show the total $n$-$^3$He cross section as a function of energy. Again we find an agreement with data that, depending on the potential, is either similar (INOY04) or better (N3LO and AV18) than observed in $n$-$^3$H [12]. As in $n$-$^3$H total cross section [12], the curves pertaining to AV18 and N3LO calculations exchange position at about the same excitation energy relative to the $n$-$^3$H threshold (E $\simeq$ 1.3 MeV) but now N3LO leads to the highest total cross section at low energy instead of at the resonance peak. The reason for this behavior is unclear at this time, but may reside in the relative position of the $0^-$ ($^3\mathrm{P}_0$) inelastic resonance [36] that is associated with the $0^-$ $\mathcal{T} = 0$ state at about 0.4 MeV excitation above the $n$-$^3$He threshold.

In conclusion, we show for the first time results of *ab initio* calculations involving four-nucleon reactions initiated by either $n$-$^3$He, $p$-$^3$H, and $d$-$d$. Realistic nuclear potentials are used between hadron pairs plus the Coulomb interaction between protons. Although specific observables show discrepancies with data that need further investigation, namely the inclusion of three-nucleon forces, the results give a reasonable overall description of the data for all six reactions that show an improvement relative to what is found for $\mathcal{T} = 1$ observables [12, 13]. Work is in progress to study the effect of three-nucleon forces through the inclusion of $\Delta$ degrees of freedom.

A.D. is supported by the Fundação para a Ciência e a Tecnologia (FCT) grant SFRH/BPD/14801/2003 and A.C.F. in part by the FCT grant POCTI/ISFL/2/275.

* Electronic address: deltuva@cii.fc.ul.pt

[1] S. C. Pieper *et al.*, Phys. Rev. C **64**, 014001 (2001).
[2] S. C. Pieper, K. Varga, and R. B. Wiringa, Phys. Rev. C **66**, 044310 (2002).
[3] E. Caurier *et al.*, Phys. Rev. C **66**, 024314 (2002).
[4] W. Glöckle *et al.*, Phys. Rep. **274**, 107 (1996).
[5] A. Kievsky, M. Viviani, and S. Rosati, Phys. Rev. C **64**, 024002 (2001).
[6] R. Lazauskas and J. Carbonell, Phys. Rev. C **70**, 044002 (2004); R. Lazauskas *et al.*, *ibid.* **71**, 034004 (2005).
[7] M. Viviani *et al.*, Phys. Rev. Lett. **86**, 3739 (2001).
[8] A. Deltuva, A. C. Fonseca, and P. U. Sauer, Phys. Rev. C **71**, 054005 (2005); **72**, 054004 (2005).
[9] E. O. Alt and W. Sandhas, Phys. Rev. C **21**, 1733 (1980).
[10] K. M. Nollett *et al.*, nucl-th/0612035.
[11] P. Grassberger and W. Sandhas, Nucl. Phys. **B2**, 181 (1967); E. O. Alt, P. Grassberger, and W. Sandhas, JINR report No. E4-6688 (1972).
[12] A. Deltuva and A. C. Fonseca, Phys. Rev. C **75**, 014005 (2006).
[13] A. Deltuva and A. C. Fonseca, nucl-th/0611013.
[14] A. C. Fonseca, Phys. Rev. Lett. **83**, 4021 (1999).
[15] B. M. Fisher *et al.*, Phys. Rev. C **74**, 034001 (2006).
[16] A. Deltuva and A. C. Fonseca, in preparation (2007).
[17] R. Machleidt, Phys. Rev. C **63**, 024001 (2001).
[18] R. B. Wiringa, V. G. J. Stoks, and R. Schiavilla, Phys. Rev. C **51**, 38 (1995).
[19] P. Doleschall, Phys. Rev. C **69**, 054001 (2004).
[20] D. R. Entem and R. Machleidt, Phys. Rev. C **68**, 041001(R) (2003).
[21] J. D. Seagrave, L. Cranberg, and J. E. Simmons, Phys. Rev. **119**, 1981 (1960).
[22] P. Jany *et al.*, Nucl. Phys. **A483**, 269 (1988).
[23] H. O. Klages *et al.*, Nucl. Phys. **A443**, 237 (1985).
[24] R. Kankowsky *et al.*, Nucl. Phys. **A263**, 29 (1976).
[25] J. M. Blair *et al.*, Phys. Rev. **74**, 1594 (1948).
[26] B. J. Crowe *et al.*, Phys. Rev. C **61**, 034006 (2000).
[27] M. Drosg, Nucl. Sci. Eng. **67**, 190 (1978).
[28] G. A. Jarvis, Los Alamos Scientific Lab Reports No. 2014, p. 35 (1956).
[29] W. E. Wilson, R. L. Walter, and D. B. Fossan, Nucl. Phys. **27**, 421 (1961).
[30] M. A. Doyle *et al.*, Nucl. Phys. **A371**, 225 (1981).
[31] J. J. Jarmer *et al.*, Phys. Rev. C **9**, 1292 (1974).
[32] J. M. Blair *et al.*, Phys. Rev. **74**, 1599 (1948).
[33] W. Grüebler *et al.*, Nucl. Phys. **A193**, 129 (1972).
[34] L. J. Dries *et al.*, Phys. Lett. **80B**, 176 (1979).
[35] Los Alamos Physics and Cryogenics Group, Nucl. Phys. **12**, 291 (1959).
[36] A. C. Fonseca *et al.*, Few-Body Systems **31**, 139 (2002).